

Stable carbon isotopes and levoglucosan for PM_{2.5} elemental carbon source apportionments in the largest city of Northwest China

Zhuzi Zhao^{a,b,*}, Junji Cao^{a,c,**}, Ting Zhang^a, Zhenxing Shen^d, Haiyan Ni^a, Jie Tian^d, Qiyuan Wang^a, Suixin Liu^a, Jiamao Zhou^a, Jian Gu^b, Ganzhou Shen^b

^a Key Laboratory of Aerosol Chemistry and Physics, Institute of Earth Environment, Chinese Academy of Sciences, Xi'an, Shaanxi, China

^b Research Center for Advanced Air Technology, China Yancheng Environmental Protection Science and Technology City, Jiangsu, China

^c Institute of Global Environment Change, Xi'an Jiaotong University, Xi'an, Shaanxi, China

^d Department of Environmental Science and Engineering, Xi'an Jiaotong University, Xi'an, Shaanxi, China

ARTICLE INFO

Keywords:

PM_{2.5}
Stable carbon isotopes
Source apportionment
Xi'an

ABSTRACT

Stable carbon isotopes provide information on aerosol sources, but no extensive long-term studies of these isotopes have been conducted in China, and they have mainly been used for qualitative rather than quantitative purposes. Here, 24 h PM_{2.5} samples (n = 58) were collected from July 2008 to June 2009 at Xi'an, China. The concentrations of organic and elemental carbon (OC and EC), water-soluble OC, and the stable carbon isotope abundances of OC and EC were determined. In spring, summer, autumn and winter, the mean stable carbon isotope in OC ($\delta^{13}\text{C}_{\text{OC}}$) were -26.4 ± 0.6 , -25.8 ± 0.7 , -25.0 ± 0.6 and $-24.4 \pm 0.8\text{‰}$, respectively, and the corresponding $\delta^{13}\text{C}_{\text{EC}}$ values were -25.5 ± 0.4 , -25.5 ± 0.8 , -25.2 ± 0.7 and $-23.7 \pm 0.6\text{‰}$. Large $\delta^{13}\text{C}_{\text{EC}}$ and $\delta^{13}\text{C}_{\text{OC}}$ values in winter can be linked to the burning coal for residential heating. Less biomass is burned during spring and summer than winter or fall (manifested in the levels of levoglucosan, i.e., 178, 85, 370, 935 ng m⁻³ in spring, summer, autumn, and winter), and the more negative $\delta^{13}\text{C}_{\text{OC}}$ in the warmer months can be explained by the formation of secondary organic aerosols. A levoglucosan tracer method combined with an isotope mass balance analysis indicated that biomass burning accounted for 1.6–29.0% of the EC, and the mean value in winter ($14.9 \pm 7.5\%$) was 7 times higher than summer ($2.1 \pm 0.4\%$), with intermediate values of 6.1 ± 5.6 and $4.5 \pm 2.4\%$ in autumn and spring. Coal combustion accounted for $45.9 \pm 23.1\%$ of the EC overall, and the percentages were 63.0, 37.2, 36.7, and 33.7% in winter, autumn, summer and spring respectively. Motor vehicles accounted for $46.6 \pm 26.5\%$ of the annual EC, and these contributed over half (56.7–61.8%) of the EC in all seasons except winter. Correlations between motor vehicle-EC and coal combustion-EC with established source indicators (B(ghi)P and As) support the source apportionment results. This paper describes a simple and accurate method for apportioning the sources of EC, and the results may be beneficial for developing model simulations as well as controlling strategies in future.

1. Introduction

Carbonaceous aerosols are important component of fine particulate matter (PM_{2.5}, particles $\leq 2.5 \mu\text{m}$ in diameter), and carbon-containing compounds concentrations can reach 20%–30% of the PM_{2.5} mass in urban China (Cao et al., 2012). Carbonaceous aerosols are typically classified into organic carbon (OC) and elemental carbon/black carbon (EC/BC). In general, EC is a primary pollutant derived exclusively from the incomplete combustion of carbon-containing substances, especially fossil fuels and biofuels, and from forest and agricultural fires and other combustion related sources (Bond et al., 2013; Jacobson, 2001). In

contrast, OC is a complex mixture of primary OC (POC) and secondary OC (SOC), which can be directly emitted from various combustion processes or produced from atmospheric reactions involving gaseous organic precursors (Pöschl, 2005; Turpin and Huntzicker, 1995). More than simply being components of PM_{2.5}, carbonaceous aerosols can substantially affect climate, air quality, visibility and impact human health. While it is important to investigate the spatial and temporal variations in these particles, they are derived from a variety of sources that can change over space and time, and as a result it can be challenging to identify their sources and even harder to quantify the impacts (Liu et al., 2013). This has led researchers to use increasingly

* Corresponding author. Key Laboratory of Aerosol Chemistry and Physics, Institute of Earth Environment, Chinese Academy of Sciences, Xi'an, Shaanxi, China.

** Corresponding author. Key Laboratory of Aerosol Chemistry and Physics, Institute of Earth Environment, Chinese Academy of Sciences, Xi'an, Shaanxi, China.

E-mail addresses: zhaozz@ieecas.cn (Z. Zhao), jjcao@ieecas.cn (J. Cao).

sophisticated models or combined methods to quantify the contributions of individual sources to the aerosol populations.

For source apportionment studies, receptor-oriented models (positive matrix factorization models (PMF), chemical mass balance models (CMB) and UNMIX, etc.), source-specific marker method (also called Aethalometer method, quantified contributions based on light absorption coefficient in the earlier study by Sandradewi et al. (2008), but not confined to the Aethalometer data only) and various multivariate models are the conventional techniques. Among these, receptor models have been in broad use for the source types quantification/assessment works, which facilitate the source contributions based on atmospheric concentrations. The marker methods (e.g., levoglucosan or stable carbon isotopes/radiocarbon, etc.) are advantageous from the point of view that they do not require many samples or extensive data sets and are quite straightforward (Salma et al., 2017; Szidat et al., 2006).

Ratios of stable carbon isotopes measured as delta- ^{13}C ($\delta^{13}\text{C}$, see below for formula) can provide information about the sources of aerosols, and these isotopes have proven to be useful geochemical markers (López-Veneroni, 2009; Widory, 2006), while radiocarbon (^{14}C) provides information on the influence of fossil fuel, biomass burning and biogenic emissions on carbonaceous aerosols (Andersson et al., 2015; Szidat et al., 2006). In particular, they have been applied in various types of environmental studies to identify emission sources (Andersson et al., 2015; Cao et al., 2011, 2013; Kawashima and Haneishi, 2012; Liu et al., 2013; Salma et al., 2017; Zhang et al., 2015). For example, measurements of $\delta^{13}\text{C}$ in both OC and EC, led Cao et al. (2013) to conclude that fossil fuel combustion was the dominant source for carbonaceous $\text{PM}_{2.5}$ in Shanghai. Earlier studies by Cao et al. (2011) using the same approach showed that northern cities in China were strongly impacted by coal combustion during winter. To date, measurements of carbon isotopes and other substances have been combined to provide new insights into characteristics of atmospheric aerosols from different sources. For example, levoglucosan (1,6-anhydro- β -D-glucopyranose), which is a sugar anhydride produced during the combustion of cellulose (Simoneit et al., 1999), is a marker commonly used to indicate biomass burning (Liu et al., 2013). Some studies coupled ^{14}C and levoglucosan marker method for source apportionment of carbonaceous aerosols (Andersson et al., 2015; Liu et al., 2013, 2017; Salma et al., 2017). Some $\delta^{13}\text{C}$ studies have conducted during biomass burning episodes, and based on the assumption that the aerosols were only affected by biomass burning, it was possible to estimate the contributions from the burning of C3 versus C4 plants to the fine PM (Cao et al., 2016; Mkoma et al., 2014). Although source apportionments based on $\delta^{13}\text{C}$ data hold considerable promise, this approach is still being developed.

Xi'an, the largest city in northwest China, is located on the Guanzhong Plain, which is surrounded by Qingling Mountains to the south and loess plateau to the north. Recently, Xi'an has experienced some of the worst air pollution among China's cities (Cao et al., 2012). The Guanzhong Plain is one of the major agricultural production areas for wheat and corn in China, and agricultural biomass burning (especially the post-harvest burning of crop residues to clear farmland) and the burning of biomass for domestic purposes are common sources of pollutants in this region, especially in autumn and winter. Previous work showed that biomass burning contributed to 5.1–43.8% of the OC in Xi'an (Zhang et al., 2014a). In addition to biomass burning, emissions from the combustion of fossil fuels, such as coal, gasoline, and diesel, are among the major sources for the carbonaceous aerosols. For example, Cao et al. (2005) found that 44% of the total carbon was from the exhaust emitted by gasoline engines, and 44% was from coal burning during winter; these results were based on absolute principal component analysis of eight thermally-derived carbon fractions.

Although studies on stable carbon isotope analysis of aerosol have been conducted at several sites in China (Cao et al., 2011, 2013, 2016; Dai et al., 2015), no extensive, long-term observations have been made, and to this point, stable carbon isotope analyses of atmospheric

particles have been used more for qualitative studies of sources rather than quantitative analysis. Here, we measured the concentrations of selected carbonaceous components and the stable carbon isotope abundances of OC and EC in $\text{PM}_{2.5}$ collected in Xi'an over an entire year. The objectives of this study were (1) to investigate seasonal variations of OC, EC, WSOC as well as stable carbon isotope composition; (2) to develop a combined ^{13}C stable isotope and levoglucosan tracer method in source apportionment for EC; and (3) to quantitatively apportion the contributions from different sources for EC mass loadings using this method and to characterize the seasonal changes in impacts from these sources.

2. Experimental

2.1. Sampling site and sample collection

The sampling site was located in the southeastern part of downtown Xi'an (34.23°N, 108.88°E) where there were no major industrial or constructive activities nearby. More detailed descriptions of the site may be found in previous publications (Xu et al., 2012; Zhang et al., 2014a). An air sampler (Model TE-6001-2.5-I- $\text{PM}_{2.5}$ SSI, Tisch Inc., USA) was deployed on the rooftop of the Institute of Earth Environment, Chinese Academy of Sciences, ~10 m above ground level. A total of 58 $\text{PM}_{2.5}$ filter samples were collected from July 2008 to June 2009. The high-volume air sampler operated at a flow rate of $1.1 \text{ m}^3 \text{ min}^{-1}$, and the sample substrates were $20 \times 25 \text{ cm}$ QM-A quartz-fiber filters (Whatman Ltd., Maidstone, UK), which were preheated in 900°C muffle furnace for at least 3 h to avoid inherent carbonaceous contaminants before using. Samples were collected every sixth day starting at 10:00 China standard time (UTC+8), and each sample was run for 24 h.

Based on the meteorological characteristics and the dates of the traditional residential heating period (mid-November through mid-March), the period from 15 November to 14 March was designated as winter, spring was 15 March to 31 May, summer was 1 June to 31 August, and autumn was 1 September to 14 November (Zhang et al., 2014a,b). In addition, four filed blank filters in each season were collected by exposing filters in the sampler without drawing air through them; these were used to account for any artifacts introduced during the sample handling process.

2.2. Carbon and stable isotope analyses

Portions of the quartz filters (0.526 cm^2 punches) were analyzed for OC and EC using a DRI Model 2001 thermal/optical carbon analyzer (Atmoslytic Inc., USA) following the IMPROVE_A protocol (Chow et al., 2007). The method detection limits (MDLs) for OC and EC were below 0.41 and $0.03 \mu\text{g cm}^{-2}$, respectively. Replicate measurements were made for one in ten samples, and the difference between replicates was < 10% for both OC and EC. Quality assurance/quality control (QA/QC) procedures for these analyses have been described by Cao et al. (2003).

Another aliquot of the sample filters was extracted with 30 mL pure water under ultrasonic agitation/extraction for three times, and filtered through a polytetrafluoroethylene filter to remove the particles and filter debris. The water extract was analyzed for water-soluble organic carbon (WSOC) using a TOC-L CPH Total Carbon Analyzer (Shimadzu Corp., Japan). The difference between OC and WSOC was considered as water-insoluble OC (WIOC).

The stable carbon isotope composition of OC and EC was determined from carbon dioxide (CO_2) evolving at two temperatures and detected with a Finnigan MAT-251 ratio mass spectrometer (Thermo Electron Corporation, Burlington, ON, Canada). The isolation of OC and EC in the study followed up by our previous studies (Cao et al., 2011; Ho et al., 2006). Briefly, the particulate carbon captured on the quartz-fiber filters was oxidized to CO_2 with CuO catalyst grains by first combusted at 375°C for 3 h (no oxygen under vacuum). The CO_2

collected by a series of cold traps, and then its isotopic composition determined as $\delta^{13}\text{C}_{\text{OC}}$. Isolation of EC was achieved by combustion of the remaining carbonaceous material at 850 °C for 5 h; the CO_2 produced by this treatment was quantified as the EC fraction and its isotopic composition defined as $\delta^{13}\text{C}_{\text{EC}}$. The EC recovery for ^{13}C measurement in this work was $123 \pm 8\%$. The positive EC artifact was probably due to OC charring during OC removal procedure before EC isolation.

The isotopic abundances were expressed relative to the international standard Vienna Pee Dee Belemnite (V-PDB) as follows:

$$\delta^{13}\text{C} = \left(\frac{^{13}\text{C}/^{12}\text{C}_{\text{sample}}}{^{13}\text{C}/^{12}\text{C}_{\text{standard}}} - 1 \right) \times 1000$$

V-PDB is the primary reference material for measuring natural variations of ^{13}C , and it is composed of calcium carbonate from a cretaceous belemnite rostrum of the Pee Dee Formation in South Carolina, USA. Samples were analyzed at least in duplicate, and the maximum difference in carbon isotopes between replicates was 0.3‰.

All the data reported here were corrected by the four field blanks.

2.3. Analysis of chemical tracers

Analysis details for levoglucosan have been reported in our previous paper (Zhang et al., 2014a,b). Briefly, aliquot of $\text{PM}_{2.5}$ samples were extracted with 10 mL Milli-Q water under ultrasonication, and filter through 0.45 μm pore size microporous membranes to remove insoluble material, then measured using high-performance anion-exchange chromatography with pulsed amperometric detector (HPAEC-PAD) on a Dionex DX-600 ion chromatograph (Dionex Inc., Sunnyvale, CA, USA). Data about levoglucosan have been reported by Zhang et al. (2014a) and cited here to evaluate biomass burning contributions to EC.

The concentrations of chemical tracers (arsenic(As) and benzo[ghi]perylene(B(ghi)P)) were determined for the $\text{PM}_{2.5}$ samples as follows. Energy dispersive X-ray fluorescence (ED-XRF) spectrometry (Epsilon 5 XRF analyzer, PANalytical, Almelo, the Netherlands) was used to determine the concentrations of the As collected on the $\text{PM}_{2.5}$ quartz-fiber filters. The analytical details and QC/QA procedures have been described in Xu et al. (2012). The accuracies and precisions of the ED-XRF analyses have been reported in previous publications (Cao et al., 2012; Xu et al., 2012). Thermal desorption (TD) coupled with gas chromatography/mass spectrometry (GC/MS) was used for quantifying the concentrations of B(ghi)P in the $\text{PM}_{2.5}$ samples. The in-injection port TD-GC/MS procedure that was used in our study involves a short sample preparation time (< 1 min), avoids contamination from solvent impurities, and is highly sensitive (Ho et al., 2008, 2011; Ho and Yu, 2004). QA/QC information for our TD-GC/MS methods may be found in Xu et al. (2013).

3. Results and discussion

3.1. Seasonal variations and concentrations of carbonaceous components

Fig. 1 presents the temporal variations in the concentrations of WSOC, WIOC and EC as well as the $\delta^{13}\text{C}$ for OC and EC at Xi'an. The seasonal variations in the concentrations of carbonaceous components are summarized in Table 1. The grand mean concentrations of WSOC, WIOC, OC and EC were 9.2 ± 6.8 , 13 ± 12 , 22 ± 17 and $7.6 \pm 3.0 \mu\text{g m}^{-3}$, and they ranged from 2.1 to 36, 1.0 to 50, 3.3 to 67 and 2.0–16 $\mu\text{g m}^{-3}$, respectively. The WSOC abundance contributes $\sim 48\% \pm 17\%$ of OC at Xi'an, and shows strong dependence on OC ($R^2 = 0.62$, $p < 0.001$) with all data points falling on a linear regression with a slope of 0.39. Although the concentrations varied significantly among samples, a seasonal pattern was observed; that is, the maximum in carbonaceous components occurred in the winter, followed by autumn, with relatively low levels in spring and summer. For example, the concentrations of WSOC, OC and EC were 1.5–3 times higher in winter

than in summer. The high loadings of carbonaceous components in winter could be explained by 1) more emissions from burning sources in the colder months coupled with meteorological conditions that led to the buildup of pollutants in the boundary layer; and 2) the emission sources, especially biomass burning for heating, residential and commercial coal combustion, etc. changed from season-to-season (manifested in the levels of levoglucosan: levoglucosan concentrations in winter were ten times higher than those in summer).

3.2. Stable carbon isotopes distribution

The daily mean isotope abundances of OC and EC were -25.3‰ and -24.9‰ , and they ranged from -27.4‰ to -23.2‰ and -26.5‰ to -22.8‰ , respectively. The mean values for $\delta^{13}\text{C}_{\text{OC}}$ and $\delta^{13}\text{C}_{\text{EC}}$ were similar to the values reported for winter and summer samples from seven northern Chinese cities in 2003 (mean value of $\delta^{13}\text{C}_{\text{OC}}$ and $\delta^{13}\text{C}_{\text{EC}}$: -25.5 and -25.1‰) (Cao et al., 2011); $\text{PM}_{2.5}$ $\delta^{13}\text{C}_{\text{EC}}$ in Akita, Japan (-24.3‰) (Kawashima and Haneishi, 2012); and $\text{PM}_{2.1}$ $\delta^{13}\text{C}_{\text{EC}}$ in Tokyo, Japan (-25.1‰) (Takahashi et al., 2008). On the other hand, the $\delta^{13}\text{C}_{\text{OC}}$ and $\delta^{13}\text{C}_{\text{EC}}$ were larger than the values measured in seven southern Chinese cities (-26.0‰ and -25.8‰) (Cao et al., 2011), British Columbia, Canada (-26.3‰ and -26.7‰) (Huang et al., 2006) and $\text{PM}_{2.5}$ $\delta^{13}\text{C}_{\text{EC}}$ in Hangzhou and Hong Kong, China (Ho et al., 2006; Liu et al., 2007). Comparisons of the isotope abundances in this study with the signatures of likely sources, show that the $\delta^{13}\text{C}_{\text{EC}}$ was close to that reported for emissions from motor vehicles (-24.9‰ to -20.3‰) (Kawashima and Haneishi, 2012) and coal combustion (-24.4‰ to -23.3‰) (Kawashima and Haneishi, 2012; Mori et al., 1999; Widory et al., 2004). Furthermore, the $\delta^{13}\text{C}_{\text{EC}}$ in the Xi'an samples was heavier than in emissions from C3 plant combustion (e.g., rice: -29.5‰ to -27.5‰) (Liu et al., 2014) but lighter than the values for C4 plants (e.g., maize: -22.2 to -13.0‰) (Liu et al., 2014). These comparisons suggest that the $\delta^{13}\text{C}_{\text{EC}}$ in our samples primarily reflected emissions from motor vehicles and coal combustion.

Notable differences were observed in the seasonality of the carbon isotopes (Fig. 2); that is, both $\delta^{13}\text{C}_{\text{OC}}$ and $\delta^{13}\text{C}_{\text{EC}}$ were clearly more enriched with ^{13}C in winter compared with the other seasons. For $\delta^{13}\text{C}_{\text{OC}}$, the values decreased in the following order: winter ($-24.4\text{‰} \pm 0.8\text{‰}$) > autumn ($-25.0\text{‰} \pm 0.6\text{‰}$) > summer ($-25.8\text{‰} \pm 0.7\text{‰}$) > spring ($-26.4\text{‰} \pm 0.6\text{‰}$); while $\delta^{13}\text{C}_{\text{EC}}$ showed enrichments of the larger ^{13}C isotope in winter ($-23.7\text{‰} \pm 0.6\text{‰}$) and similar ratios in spring ($-25.5\text{‰} \pm 0.4\text{‰}$), summer ($-25.5\text{‰} \pm 0.8\text{‰}$) and autumn ($-25.3\text{‰} \pm 0.7\text{‰}$). Normally, EC is unreactive, and therefore $\delta^{13}\text{C}_{\text{EC}}$ is likely to preserve the characteristics of the primary sources (Huang et al., 2006). Differences in the mean winter $\delta^{13}\text{C}_{\text{EC}}$ values versus other seasons indicate that the major sources for EC from Xi'an change with season. In northern China, large quantities of coal are burned for residential heating, and the so-called heating season extends from November of one year to March of the following year (Cao et al., 2007). The larger values of $\delta^{13}\text{C}_{\text{EC}}$ as well as $\delta^{13}\text{C}_{\text{OC}}$ we observed in winter relative to other seasons might be linked to the burning of coal for residential heating.

In contrast to EC, the OC fraction of the aerosol can be modified by various reactions, and as a result, $\delta^{13}\text{C}_{\text{OC}}$ values typically change with time (Cao et al., 2011). Indeed, photochemical reactions and the accumulation of biogenic materials can both lead to lighter $\delta^{13}\text{C}_{\text{OC}}$ (Ho et al., 2006), and a study by Irei et al. (2006) showed that the $\delta^{13}\text{C}$ of secondary organic aerosol (SOA) produced in laboratory studies was light, ranging from -32.2‰ to -32.9‰ . Along these lines, we found higher percentages of WSOC in OC in spring (55%) and summer (52%) compared with autumn (40%) or winter (46%) (Table 1). Generally, WSOC is associated with polar compounds, SOA formation, and biomass burning-derived POC (Ding et al., 2008). Due to the relatively low levels of biomass burning emissions during spring and summer, which can be seen in the seasonality of levoglucosan concentrations (spring = 178 ng m^{-3} ; summer = 85 ng m^{-3} ; autumn = 370 ng m^{-3} ;

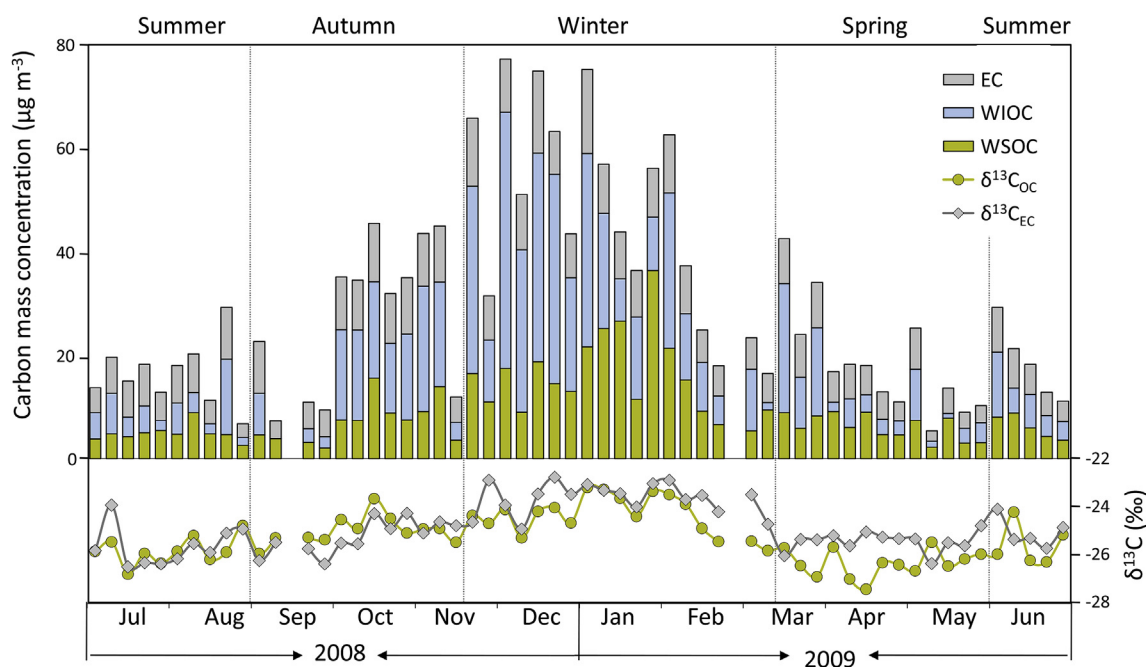


Fig. 1. Temporal variations in the mass concentrations of carbonaceous aerosol components, including water-soluble and water-insoluble organic carbon (WSOC and WIOC), elemental carbon (EC) and delta ^{13}C ($\delta^{13}\text{C}$) for OC and EC.

winter = 935 ng m^{-3}), we can conclude that the high WSOC fraction is indicative of aged aerosols. And thus, the more negative $\delta^{13}\text{C}_{\text{OC}}$ in the planting and growing seasons can be explained by the formation SOA with the higher percentage of the lighter ^{12}C isotope (See Fig. 3).

A plot of $\delta^{13}\text{C}_{\text{OC}}$ versus $\delta^{13}\text{C}_{\text{EC}}$ shows that the stable C ratios of OC and EC were moderately correlated over the whole year ($R^2 = 0.47$, $p < 0.001$); however, when the samples were grouped by season, the correlation between $\delta^{13}\text{C}_{\text{OC}}$ and $\delta^{13}\text{C}_{\text{EC}}$ decreased in winter and autumn ($R^2 = 0.38$ and 0.36 , respectively) and became non-significant ($p > 0.05$) in spring ($R^2 = 0.18$) and summer ($R^2 = 0.19$). Assuming that EC maintains the isotopic signature ($\delta^{13}\text{C}_{\text{EC}}$) of the original emissions, one can conclude that the isotopic composition of OC was at times affected by the same combustion sources as EC, especially coal combustion during the winter heating season and the postharvest burning of crop residues in autumn. In spring and summer, there was no correlation between $\delta^{13}\text{C}_{\text{OC}}$ and $\delta^{13}\text{C}_{\text{EC}}$, however, and that was most likely due to the formation of SOA and the attendant effects on $\delta^{13}\text{C}_{\text{OC}}$.

3.3. Source apportionment of EC

3.3.1. Biomass burning EC

Atmospheric processing and photochemical aging affect the $\delta^{13}\text{C}$ signature of OC but not EC, and this is why $\delta^{13}\text{C}_{\text{EC}}$ was the focus in our

assessment of the emission sources. More specifically, EC is chemically stable, and carbon isotopic fractionation of EC does not occur easily in nature (Liu et al., 2014), and thus $\delta^{13}\text{C}_{\text{EC}}$ provides information on emission sources (Andersson et al., 2015). For our quantitative mass-balance source-apportionments for EC, three main combustion source fuels were assumed, and these were biomass, coal and liquid fossil fuels. This strategy is based on two principles; first, these sources account for the bulk of the BC emissions in China, and second, these sources can be distinguished by analyses of stable carbon isotopes. Here, the carbon isotope mass balance approach was combined with a levoglucosan tracer method to estimate the relative contributions of various sources to EC.

Levoglucosan to EC ratios have been used to assess impacts from biomass burning, and previous studies have used a levoglucosan tracer method to evaluate the impacts of biomass burning on OC (Sang et al., 2011; Zhang et al., 2014a). Here, equation (1), which is based on an enrichment factor receptor modeling approach, was adapted and applied to estimate the contribution of biomass burning to EC

$$\text{Contribution of biomass burning to EC} = \frac{[\text{Levoglucosan}]/[\text{EC}]_{\text{ambient}}}{[\text{Levoglucosan}]/[\text{EC}]_{\text{source}}} \quad (1)$$

The implicit assumptions of this approach are (1) that levoglucosan

Table 1

Annual and seasonal mean \pm SD (median) concentrations of WSOC, WIOC, OC, EC, levoglucosan and $\delta^{13}\text{C}$ for $\text{PM}_{2.5}$ from Xi'an.

| Variable | Season | | | | Annual |
|--|-------------------------|-------------------------|-------------------------|-------------------------|-------------------------|
| | Spring | Summer | Autumn | Winter | |
| Number of samples | 13 | 15 | 12 | 18 | 58 |
| WSOC ($\mu\text{g m}^{-3}$) | 6.1 ± 2.5 (6.0) | 5.3 ± 1.9 (4.8) | 7.5 ± 4.3 (7.4) | 16 ± 8.0 (15) | 9.3 ± 6.8 (7.5) |
| WIOC ($\mu\text{g m}^{-3}$) | 6.7 ± 7.1 (3.4) | 5.6 ± 3.7 (4.9) | 13 ± 7.8 (17) | 22 ± 14 (19) | 13 ± 12 (8.2) |
| OC ($\mu\text{g m}^{-3}$) | 13 ± 8.5 (11) | 11 ± 4.6 (10) | 21 ± 12 (24) | 38 ± 18 (38) | 22 ± 17 (16) |
| EC ($\mu\text{g m}^{-3}$) | 5.7 ± 2.3 (5.7) | 6.3 ± 2.0 (7.0) | 8.4 ± 2.9 (10) | 9.6 ± 3.1 (9.1) | 7.6 ± 3.0 (8.0) |
| levoglucosan (ng m^{-3}) ^a | 178 ± 125 (97) | 85 ± 24 (87) | 370 ± 325 (176) | 935 ± 443 (872) | 428 ± 399 (156) |
| WSOC/OC (%) | 55 ± 19 (52) | 52 ± 14 (50) | 40 ± 10 (40) | 46 ± 19 (42) | 48 ± 17 (48) |
| $\delta^{13}\text{C}_{\text{OC}}$ (‰) | -26.4 ± 0.6 (-26.4) | -25.8 ± 0.7 (-25.5) | -25.0 ± 0.6 (-25.0) | -24.4 ± 0.8 (-24.3) | -25.3 ± 1.0 (-25.4) |
| $\delta^{13}\text{C}_{\text{EC}}$ (‰) | -25.5 ± 0.4 (-25.4) | -25.5 ± 0.8 (-25.9) | -25.2 ± 0.7 (-25.3) | -23.7 ± 0.6 (-23.5) | -24.9 ± 1.0 (-25.1) |

^a Data obtained from Zhang et al. (2014a).

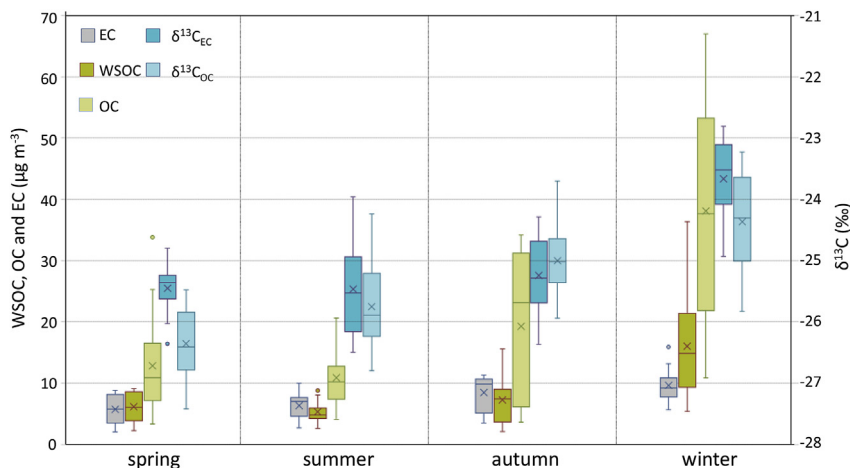


Fig. 2. Box plots of OC, EC, WSOC concentrations ($\mu\text{g m}^{-3}$) as well as $\delta^{13}\text{C}_{\text{OC}}$, $\delta^{13}\text{C}_{\text{EC}}$ (‰) in $\text{PM}_{2.5}$ in four seasons. Boxes and whiskers represent the minimum value, 25th, 50th, 75th percentiles and maximum value. The X sign in the middle of the boxes show the mean values for each component.

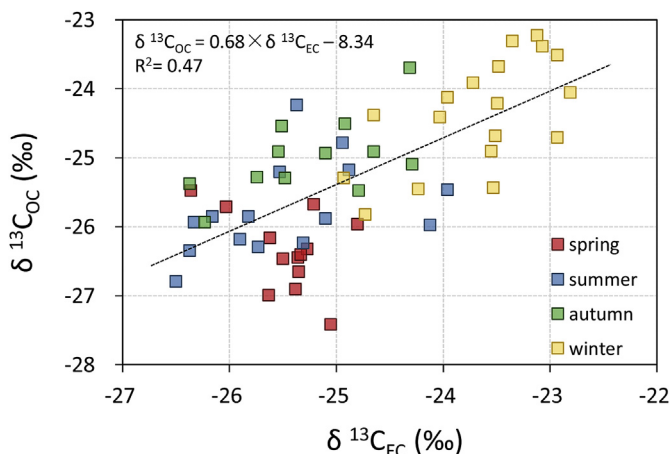


Fig. 3. Relationships between stable carbon isotope ratios ($\delta^{13}\text{C}_{\text{EC}}$ and $\delta^{13}\text{C}_{\text{OC}}$) in $\text{PM}_{2.5}$ in four seasons. The diagonal line shows the linear regression.

can be used as a tracer for separating biomass burning impacts from those of other sources, but (2) it cannot be used to distinguish among different biomass fuels and combustion sources. With reference to the levoglucosan/EC ratios of likely sources materials, Zhang et al. (2007) reported an average of 7.69% (with a range of 5.4–11.8%) for cereal straw (corn, wheat, and rice) in China. Due to the lack of information

on the composition of emissions from different types of biomass under realistic burning scenarios, we used this value in our calculations. Using this approach, the percent contribution of biomass burning to EC in fine particles for the daily samples was found to vary from 1.6% to 29% over the course of the sampling campaign and averaged $7.4 \pm 7.2\%$ (Fig. 4). The average percent contribution in winter ($15 \pm 7.5\%$) was seven times higher than in summer ($2.1 \pm 0.4\%$), and the percentages were $6.1 \pm 5.6\%$ and $4.5 \pm 2.4\%$ for autumn and spring, respectively.

3.3.2. Coal combustion EC and motor vehicle EC

Based on the “Aethalometer method” principle, if one assumes that the influence of mineral dust on EC is negligible, the relative contributions of biomass burning, coal combustion and motor vehicle exhaust can be estimated using the isotope mass balance approach for $\delta^{13}\text{C}_{\text{EC}}$. Again, the focus here is on EC because that is the carbonaceous aerosol fraction that retains the original signature of the primary emissions. The mass balance model for $\delta^{13}\text{C}_{\text{EC}}$ is as follows:

$$\delta^{13}\text{C}_{\text{EC AM}} = a\delta^{13}\text{C}_{\text{EC CC}} + b\delta^{13}\text{C}_{\text{EC MV}} + c\delta^{13}\text{C}_{\text{EC BB}} \quad (2)$$

where $\delta^{13}\text{C}_{\text{EC AM}}$ is the $\delta^{13}\text{C}_{\text{EC}}$ measured in ambient samples (here $\text{PM}_{2.5}$), $\delta^{13}\text{C}_{\text{EC CC}}$ is the $\delta^{13}\text{C}_{\text{EC}}$ representative of coal combustion (CC), $\delta^{13}\text{C}_{\text{EC MV}}$ is the $\delta^{13}\text{C}_{\text{EC}}$ of motor vehicle (MV) exhaust, $\delta^{13}\text{C}_{\text{EC BB}}$ is the $\delta^{13}\text{C}_{\text{EC}}$ of biomass burning (BB), and a, b, and c denote the percent contributions from CC, MV and BB; note that $a + b + c = 1$. The value for c for each sample was obtained from Eq. (1).

This approach can be refined to take into account differences in

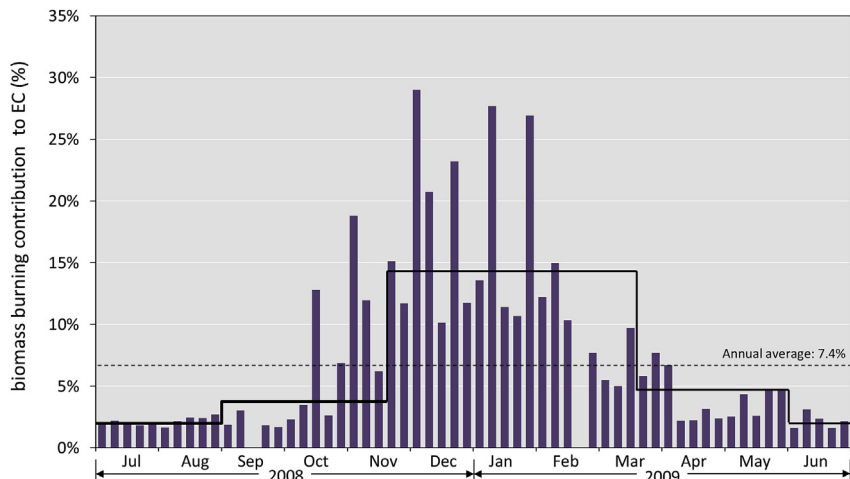


Fig. 4. Daily contributions of biomass burning to EC (calculation based on the levoglucosan tracer method). The solid line shows the seasonal mean values.

terrestrial vegetation, that is, to account for the fact that C3, C4 and CAM plants show differences in isotope discrimination (Sage, 2004). To do this, we first collected productivity figures for the staple crops (rice, wheat and maize) in 2008 and 2009 for Shaanxi Province from Shaanxi Statistical Yearbook (Table S2). The average yields of rice, wheat, and maize in 2008 and 2009 combined were 0.83, 3.87 and 5.05 million tons, respectively, and these three crops accounted for nearly 84% of the total crop production. If one assumes that biomass burning emissions are dominated by these three crops, then we can estimate their contributions to biomass burning separately based on their production figures, and to do this, Eq. (2) was revised as follows:

$$\delta^{13}\text{C}_{\text{EC AM}} = a\delta^{13}\text{C}_{\text{EC CC}} + b\delta^{13}\text{C}_{\text{EC MV}} + c(C_{\text{rice}}\delta^{13}\text{C}_{\text{EC rice}} + C_{\text{wheat}}\delta^{13}\text{C}_{\text{EC wheat}} + C_{\text{maize}}\delta^{13}\text{C}_{\text{EC maize}}) \quad (3)$$

where $\delta^{13}\text{C}_{\text{EC rice}}$, $\delta^{13}\text{C}_{\text{EC wheat}}$, $\delta^{13}\text{C}_{\text{EC maize}}$ denote the $\delta^{13}\text{C}_{\text{EC}}$ values for rice, wheat and maize, respectively, and C_{rice} , C_{wheat} and C_{maize} are the percent contributions from rice, wheat and maize to biomass burning.

For these calculations, we used $\delta^{13}\text{C}_{\text{EC}}$ values matched to these three crops that were taken from a paper by Liu et al. (2014). These authors collected six cultivars of rice, maize, and wheat, burned the residues under both flaming and smoldering conditions, and then determined the carbon isotopic ratios for EC in smoke and ash. The $\delta^{13}\text{C}$ values were relatively similar for rice (−29.5 and −27.5‰) and wheat (−29.9 and −25.4‰) while those for maize were somewhat larger (−22.2 and −13.0‰). To allow for the uncertainties in these isotopic values, three calculations were done here. The first using the mean $\delta^{13}\text{C}$ values for all three crops, the second with the lower values and the third with the upper values.

For the coal combustion products and motor vehicle exhaust, we considered the $\delta^{13}\text{C}$ values reported in several relevant publications (Mori et al., 1999; Widory, 2006; Huang et al., 2006; Kawashima and Haneishi, 2012), and finally adopted values of −23.3‰ for coal and −26.9‰ for motor vehicle for use in Eq. (3). The $\delta^{13}\text{C}$ values for EC for selected atmospheric pollution sources are listed in Table S1. Thus, based on the selected $\delta^{13}\text{C}$ values, we could establish binary equations to apportion the source contributions for each sample.

The temporal source apportionment of EC for the set of 24 h samples collected from July 2008 to June 2009 indicates that coal combustion accounted for $46 \pm 23\%$ of the EC (Fig. 5) on average, and its contribution was highest in winter ($63 \pm 18\%$), similar in autumn ($37 \pm 16\%$) and summer ($37 \pm 21\%$) and lowest in spring ($34 \pm 13\%$). Motor vehicle emissions accounted for $47 \pm 27\%$ of annual EC mass, and it was the largest contributor to EC in spring (62%), summer (61%) and autumn (57%). The results of the source apportionments are comparable to the results for previous assessments for cities in northern China that were based on measurements of radiocarbon. For example, Zhang et al. (2015) found that the contributions of fossil fuel sources to EC was $78\% \pm 3\%$ in Xi'an in January 2013. Chen et al. (2013) found that 83–86% of the EC was associated with fossil fuel combustion during winter 2009–2010 in Beijing, Shanghai and Xiamen, with the remainder from biomass burning. Andersson et al. (2015) found that coal combustion contributed 66% (46–74%) of the EC in the Beijing region in winter 2013.

3.3.3. Evaluation the apportionment results

To evaluate the validity of the stable carbon isotope-resolved source contributions, we compared the EC concentrations calculated for coal combustion and motor vehicle sources with those of established markers for these sources. The markers used for this purpose were As for coal burning and B(ghi)P for vehicular emissions. Coal combustion is one of the major sources for As in the atmosphere (Xie et al., 2006), and for each ton of permocarboniferous coal (containing roughly 5 mg kg^{-1} As) burned, power stations emit roughly 0.40 g As into the atmosphere, most of which is associated with fly ash (Luo et al., 2004). The chemical tracer we used for motor vehicles is B(ghi)P. Although B(ghi)P can be

generated by both coal and gasoline combustions, B(ghi)P is mainly from gasoline emissions (Wang et al., 2006; Xu et al., 2013). Fig. 6 shows a moderate correlation ($R^2 = 0.32$, $p < 0.001$) between the calculated coal combustion-EC and As, and this supports the conclusions we have drawn from the source apportionment regarding the contributions of this source. Interestingly, we had to separate the data into winter and other seasons (spring, summer and autumn) to obtain good correlations between B(ghi)P and motor vehicle-EC, with $R^2 = 0.44$ ($p = 0.005$) and 0.49 ($p < 0.001$) in winter and other seasons, respectively. The correlations between B(ghi)P and motor vehicle-EC did not hold for all data combined because the slopes varied among seasons. This might relate to the B(ghi)P concentrations were perturbed by the increased coal combustion in winter. Even so, the relationships between the tracers and the coal combustion-EC and motor vehicle-EC indicate that our assessment provides a reasonable representation of EC sources and concentrations at Xi'an.

3.3.4. Uncertainty estimation and limitations

Special care needs to be taken in interpreting the apportioning results because the source apportionments are dependent on the selection of the $\delta^{13}\text{C}$ reference values. The uncertainties of coal combustion and motor vehicle contributions to EC calculated in different isotopic values were estimated. When we used the lower and upper bounds of $\delta^{13}\text{C}_{\text{EC}}$ values of rice, wheat and maize in separate calculations, estimates of the annual mean contribution of coal combustion to EC were ~55% and 41%, respectively. Correspondingly, motor vehicle emissions contributed ~38% and ~52%. The seasonal contributions from coal combustion and motor vehicle exhaust emissions to EC are listed in Table S3. The overall relative uncertainty of the coal combustion contributions was assessed to be up to 10% (medians: 6.6%; range: 1.2%–45%), while the relative uncertainty for the motor vehicle contributions is expected to be ~15%. Besides that, we selected one end number of $\delta^{13}\text{C}_{\text{EC}}$ for coal combustion (−23.3‰) and motor vehicle (−26.9‰) in the calculations, while large range for $\delta^{13}\text{C}_{\text{EC}}$ from different sources have been reported in previous publications (Huang et al., 2006; Kawashima and Haneishi, 2012; Mori et al., 1999; Widory, 2006). The uncertainties were estimated by varying reference ratios by ± 0.1 . It was estimated that the relative uncertainty associated with the variations is approximately ~3%.

Meanwhile, this study has some limitations. We note that the typical uncertainties of source apportionment arise from the input parameters for calculations, including not only the variability of reference values, but also analytical uncertainties (including OC/EC mass and isotope measurements) and recoveries of different carbon fractions. Hammes et al. (2007) pointed out that the specific chemical/thermal/physical methods used to isolate the EC fraction could conceivably influence the signatures. Zhang et al. (2012) evaluated the extent of positive and negative artefacts during OC and EC separation, and then obtained the optimal strategy for subsequent off-line ^{14}C measurement which used in their recently works (Zhang et al., 2014b, 2015). Thus, the determination of these uncertainties as well as the results of the sensitivity analysis should be conducted in the future. In addition, the levoglucosan/EC ratio of 7.69% for the main types of Chinese cereal straw (Zhang et al., 2007) was chosen to evaluate the biomass burning contribution to EC, which also should be taken into account in the calculations. Nevertheless, this apportioning method provides a new chance to obtain relative contributions to EC from different sources.

4. Conclusions

PM_{2.5} samples ($n = 58$) were collected every sixth day from July 2008 to June 2009 at Xi'an, Shaanxi Province, in the interior of China. Stable carbon isotope abundances for the OC and EC fractions as well as the concentrations of carbonaceous components (OC, EC and WSOC) were determined. The larger values of $\delta^{13}\text{C}_{\text{EC}}$ and $\delta^{13}\text{C}_{\text{OC}}$ observed in winter relative to other seasons can be linked to the burning of coal for

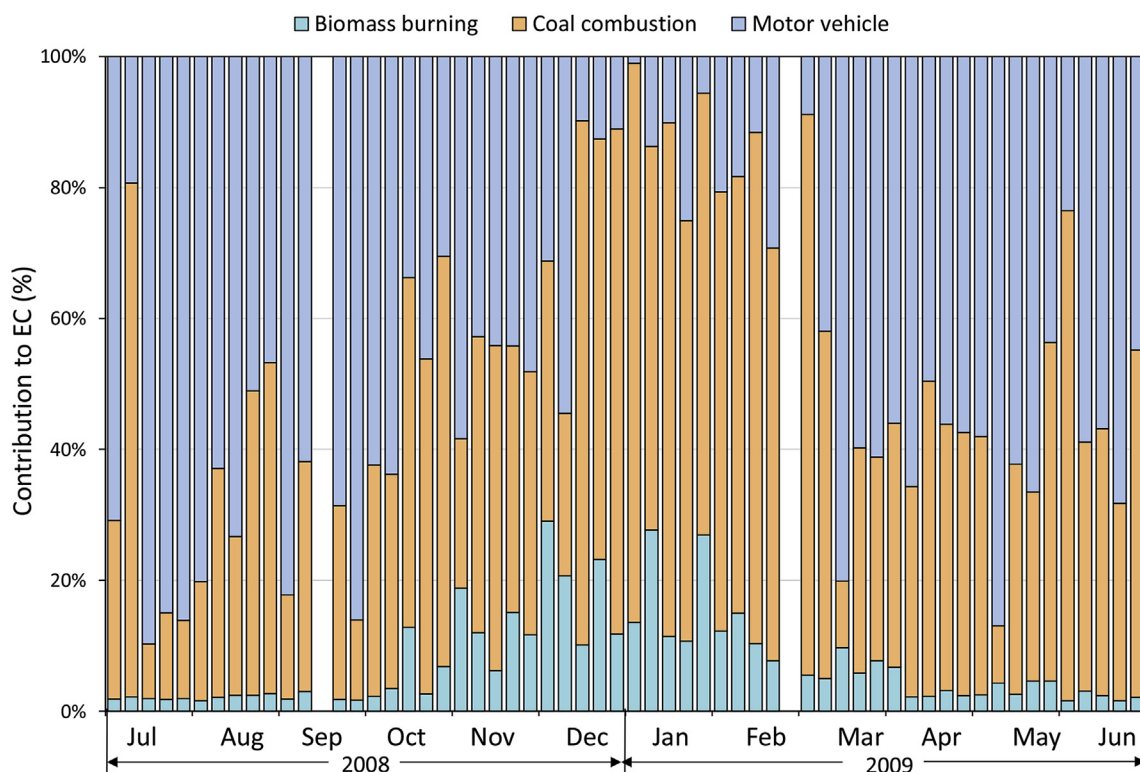


Fig. 5. Temporal source apportionment of EC from July 2008 to June 2009.

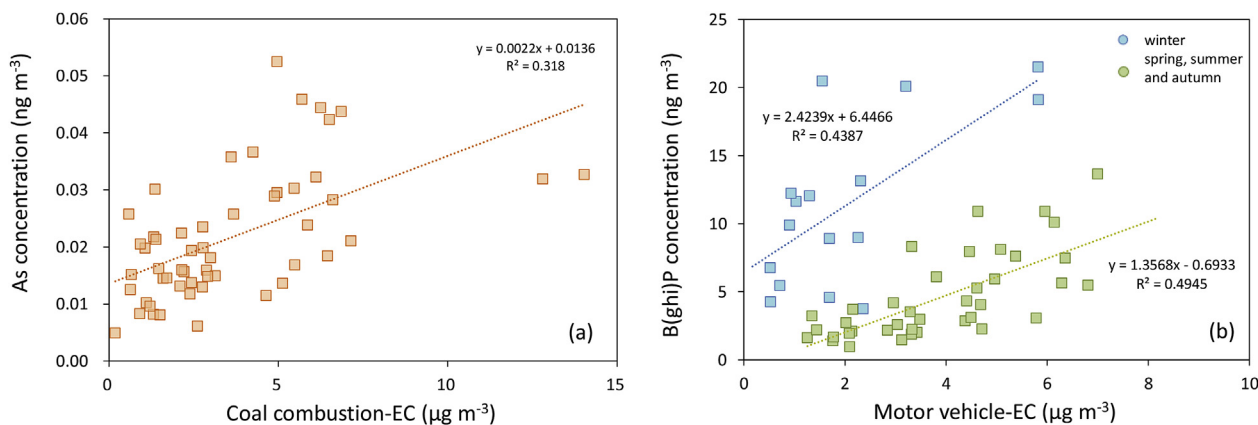


Fig. 6. Relationships between (a) arsenic and coal combustion-EC and (b) B(ghi)P and motor vehicle-EC.

residential heating. On the other hand, relatively low amounts of biomass are burned during spring and summer, so the more negative $\delta^{13}C_{OC}$ in those seasons is probably related to the formation SOA because that process favors the lighter ^{12}C isotope over ^{13}C .

We combined a levoglucosan tracer method, which has been used to estimate the impacts of biomass burning, with the isotope mass-balance approach to estimate source contributions to EC. The percent contribution of biomass burning to EC ranged from 1.6% to 29% and averaged of $7.4 \pm 7.2\%$ for the study. After accounting for the contributions of biomass burning to EC, the relative contributions of coal combustion and motor vehicle exhaust were estimated using the isotope mass balance approach for $\delta^{13}C_{EC}$. Motor vehicle emissions apparently were responsible for the greatest fraction of EC in spring, summer and autumn while coal combustion was the most important source in winter. These findings are similar to results from previous studies in northern Chinese cities that were based on measurements of radiocarbon. To assess the validity of the source contributions based on stable carbon isotopes, the EC concentrations calculated for coal

combustion and motor vehicle source were compared with those of source markers, As for coal combustion and B(ghi)P for motor vehicle emissions. Significant relationships between As and coal combustion-EC, and for B(ghi)P and motor vehicle-EC indicated that our new approach for assessing EC sources was able to provide a reasonable representation of EC sources and concentrations at Xi'an.

This is the first study to use stable C isotopes for source apportionments of EC, which provides a simple and relatively accurate apportioning method. In addition, carbonaceous aerosols are a major cause of high $PM_{2.5}$ loadings, and the findings presented here concerning sources provide a starting point for developing model simulations as well as controlling strategies in future.

Acknowledgements

This study was supported by the National Natural Science Foundation of China (41603129, 41230641) and the General Financial Grant from the China Postdoctoral Science Foundation (2016M592852).

Appendix A. Supplementary data

Supplementary data related to this article can be found at <http://dx.doi.org/10.1016/j.atmosenv.2018.05.008>.

References

- Andersson, A., Deng, J., Du, K., Zheng, M., Yan, C., Sköld, M., Gustafsson, Ö., 2015. Regionally-varying combustion sources of the January 2013 severe haze events over eastern China. *Environmental Science & Technology* 49, 2038–2043.
- Bond, T.C., Doherty, S.J., Fahey, D.W., Forster, P.M., Bernsten, T., DeAngelo, B.J., Flanner, M.G., Ghan, S., Kärcher, B., Koch, D., Kinne, S., Kondo, Y., Quinn, P.K., Sarofim, M.C., Schultz, M.G., Schulz, M., Venkataraman, C., Zhang, H., Zhang, S., Bellouin, N., Guttikunda, S.K., Hopke, P.K., Jacobson, M.Z., Kaiser, J.W., Klimont, Z., Lohmann, U., Schwarz, J.P., Shindell, D., Storelvmo, T., Warren, S.G., Zender, C.S., 2013. Bounding the role of black carbon in the climate system: a scientific assessment. *J. Geophys. Res.: Atmosphere* 118, 5380–5552.
- Cao, F., Zhang, S.-C., Kawamura, K., Zhang, Y.-L., 2016. Inorganic markers, carbonaceous components and stable carbon isotope from biomass burning aerosols in Northeast China. *Sci. Total Environ.* 572, 1244–1251.
- Cao, J., Chow, J., Tao, J., Lee, S.-C., Watson, J.G., Ho, K.F., Wang, G.-h., Zhu, C.-S., Han, Y., 2011. Stable carbon isotopes in aerosols from Chinese cities: influence of fossil fuels. *Atmos. Environ.* 45, 1359–1363.
- Cao, J., Lee, S.F., Ho, K., Zhang, X., Zou, S., Fung, K., Chow, J.C., Watson, J.G., 2003. Characteristics of carbonaceous aerosol in pearl river delta region, China during 2001 winter period. *Atmos. Environ.* 37, 1451–1460.
- Cao, J., Shen, Z., Chow, J.C., Watson, J.G., Lee, S., Tie, X., Ho, K., Wang, G., Han, Y., 2012. Winter and summer PM_{2.5} chemical compositions in fourteen Chinese cities. *J. Air Waste Manag. Assoc.* 62, 1214–1226.
- Cao, J.J., Lee, S.C., Chow, J.C., Watson, J.G., Ho, K.F., Zhang, R.J., Jin, Z.D., Shen, Z.X., Chen, G.C., Kang, Y.M., Zou, S.C., Zhang, L.Z., Qi, S.H., Dai, M.H., Cheng, Y., Hu, K., 2007. Spatial and seasonal distributions of carbonaceous aerosols over China. *J. Geophys. Res.: Atmosphere* 112, D22S11.
- Cao, J.J., Wu, F., Chow, J.C., Lee, S.C., Li, Y., Chen, S.W., An, Z.S., Fung, K.K., Watson, J.G., Zhu, C.S., Liu, S.X., 2005. Characterization and source apportionment of atmospheric organic and elemental carbon during fall and winter of 2003 in Xi'an, China. *Atmos. Chem. Phys.* 5, 3127–3137.
- Cao, J.J., Zhu, C.S., Tie, X.X., Geng, F.H., Xu, H.M., Ho, S.S.H., Wang, G.H., Han, Y.M., Ho, K.F., 2013. Characteristics and sources of carbonaceous aerosols from Shanghai, China. *Atmos. Chem. Phys.* 13, 803–817.
- Chen, B., Andersson, A., Lee, M., Kirillova, E.N., Xiao, Q., Krusá, M., Shi, M., Hu, K., Lu, Z., Streets, D.G., Du, K., Gustafsson, Ö., 2013. Source forensics of black carbon aerosols from China. *Environmental Science & Technology* 47, 9102–9108.
- Chow, J.C., Watson, J.G., Chen, L.-W.A., Chang, M.O., Robinson, N.F., Trimble, D., Kohl, S., 2007. The IMPROVE-A temperature protocol for thermal/optical carbon analysis: maintaining consistency with a long-term database. *J. Air Waste Manag. Assoc.* 57, 1014–1023.
- Dai, S., Bi, X., Chan, L.Y., He, J., Wang, B., Wang, X., Peng, P., Sheng, G., Fu, J., 2015. Chemical and stable carbon isotopic composition of PM_{2.5} from on-road vehicle emissions in the PRD region and implications for vehicle emission control policy. *Atmos. Chem. Phys.* 15, 3097–3108.
- Ding, X., Zheng, M., Yu, L., Zhang, X., Weber, R.J., Yan, B., Russell, A.G., Edgerton, E.S., Wang, X., 2008. Spatial and seasonal trends in biogenic secondary organic aerosol tracers and water-soluble organic carbon in the southeastern United States. *Environmental Science & Technology* 42, 5171–5176.
- Hammes, K., Schmidt, M.W.I., Smernik, R.J., Currie, L.A., Ball, W.P., Nguyen, T.H., Louchouart, P., Houel, S., Gustafsson, Ö., Elmquist, M., Cornelissen, G., Skjemstad, J.O., Masiello, C.A., Song, J., Peng, P., Mitra, S., Dunn, J.C., Hatcher, P.G., Hockaday, W.C., Smith, D.M., Hartkopf-Pröder, C., Böhrer, A., Lüer, B., Huebert, B.J., Amelung, W., Brodowski, S., Huang, L., Zhang, W., Gschwend, P.M., Flores-Cervantes, D.X., Largeau, C., Rouzaud, J.-N., Rumpel, C., Guggenberger, G., Kaiser, K., Rodionov, A., Gonzalez-Vila, F.J., Gonzalez-Perez, J.A., de la Rosa, J.M., Manning, D.A.C., López-Capel, E., Ding, L., 2007. Comparison of quantification methods to measure fire-derived (black/elemental) carbon in soils and sediments using reference materials from soil, water, sediment and the atmosphere. *Global Biogeochem. Cycles* 21. <http://dx.doi.org/10.1029/2006GB002914>.
- Ho, K.F., Lee, S.C., Cao, J.J., Li, Y.S., Chow, J.C., Watson, J.G., Fung, K., 2006. Variability of organic and elemental carbon, water soluble organic carbon, and isotopes in Hong Kong. *Atmos. Chem. Phys.* 6, 4569–4576.
- Ho, S.S.H., Chow, J., Watson, J., Pan Ting Ng, L., Kwok, Y., Ho, K.F., Cao, J., 2011. Precautions for in-injection port thermal desorption-gas chromatography/mass spectrometry (TD-gc/MS) as applied to aerosol filter samples. *Atmos. Environ.* 45, 1491–1496.
- Ho, S.S.H., Yu, J., Chow, J., Zielinska, B., Watson, J., Hoi Leung Sit, E., Schauer, J., 2008. Evaluation of an In-injection Port Thermal Desorption-gas Chromatography/mass Spectrometry Method for Analysis of Non-polar Organic Compounds in Ambient Aerosol Samples.
- Ho, S.S.H., Yu, J.Z., 2004. In-injection port thermal desorption and subsequent gas chromatography–mass spectrometric analysis of polycyclic aromatic hydrocarbons and n-alkanes in atmospheric aerosol samples. *J. Chromatogr. A* 1059, 121–129.
- Huang, L., Brook, J.R., Zhang, W., Li, S.M., Graham, L., Ernst, D., Chivulescu, A., Lu, G., 2006. Stable isotope measurements of carbon fractions (OC/EC) in airborne particulate: a new dimension for source characterization and apportionment. *Atmos. Environ.* 40, 2690–2705.
- Irei, S., Huang, L., Collin, F., Zhang, W., Hastie, D., Rudolph, J., 2006. Flow reactor studies of the stable carbon isotope composition of secondary particulate organic matter generated by OH-radical-induced reactions of toluene. *Atmos. Environ.* 40, 5858–5867.
- Jacobson, M.Z., 2001. Strong radiative heating due to the mixing state of black carbon in atmospheric aerosols. *Nature* 409, 695–697.
- Kawashima, H., Haneishi, Y., 2012. Effects of combustion emissions from the Eurasian continent in winter on seasonal $\delta^{13}C$ of elemental carbon in aerosols in Japan. *Atmos. Environ.* 46, 568–579.
- López-Veneroni, D., 2009. The stable carbon isotope composition of PM_{2.5} and PM₁₀ in Mexico City Metropolitan Area air. *Atmos. Environ.* 43, 4491–4502.
- Liu, D., Li, J., Cheng, Z., Zhong, G., Zhu, S., Ding, P., Shen, C., Tian, C., Chen, Y., Zhi, G., Zhang, G., 2017. Sources of Non-fossil-fuel Emissions in Carbonaceous Aerosols during Early Winter in Chinese Cities.
- Liu, D., Li, J., Zhang, Y., Xu, Y., Liu, X., Ding, P., Shen, C., Chen, Y., Tian, C., Zhang, G., 2013. The use of levoglucosan and radiocarbon for source apportionment of PM_{2.5} carbonaceous aerosols at a background site in east China. *Environmental Science & Technology* 47, 10454–10461.
- Liu, G., Li, J., Xu, H., Wu, D., Liu, Y., Yang, H., 2014. Isotopic compositions of elemental carbon in smoke and ash derived from crop straw combustion. *Atmos. Environ.* 92, 303–308.
- Liu, G., Zhang, X., Teng, W., Yang, H., 2007. Isotopic composition of organic carbon and elemental carbon in PM_{2.5} in Hangzhou, China. *Chin. Sci. Bull.* 52, 2435–2437.
- Luo, K., Zhang, X., Chen, C., Lu, Y., 2004. Estimate of arsenic emission amount from the coal power stations in China. *Chin. Sci. Bull.* 49, 2183–2189.
- Mkoma, S.L., Kawamura, K., Tachibana, E., Fu, P., 2014. Stable carbon and nitrogen isotopic compositions of tropical atmospheric aerosols: sources and contribution from burning of C3 and C4 plants to organic aerosols. *Tellus B* 66, 20176.
- Mori, I., Nishikawa, M., Quan, H., Iwasaka, Y., 1999. Regional characteristics of Chinese atmospheric aerosols in terms of the stable carbon isotope ratios [in Japanese]. In: *Japan Society on Atmospheric Environment Annual Meeting. Proceedings of Japan Society on Atmospheric Environment Annual Meeting*, pp. 419.
- Pöschl, U., 2005. *Atmospheric Aerosols: Composition, Transformation, Climate and Health Effects*.
- Sage, R.F., 2004. The evolution of C4 photosynthesis. *New Phytol.* 161, 341–370.
- Salma, I., Németh, Z., Weidinger, T., Maenhaut, W., Claeys, M., Molnár, M., Major, I., Ajtai, T., Utry, N., Bozóki, Z., 2017. Source apportionment of carbonaceous chemical species to fossil fuel combustion, biomass burning and biogenic emissions by a coupled radiocarbon–levoglucosan marker method. *Atmos. Chem. Phys.* 17, 13767–13781.
- Sandradewi, J., Prévôt, A.S.H., Szidat, S., Perron, N., Alfarra, M.R., Lanz, V.A., Weingartner, E., Baltensperger, U., 2008. Using aerosol light absorption measurements for the quantitative determination of wood burning and traffic emission contributions to particulate matter. *Environmental Science & Technology* 42, 3316–3323.
- Sang, X.-F., Chan, C.-Y., Engling, G., Chan, L.-Y., Wang, X.-M., Zhang, Y.-N., Shi, S., Zhang, Z.-S., Zhang, T., Hu, M., 2011. Levoglucosan enhancement in ambient aerosol during springtime transport events of biomass burning smoke to Southeast China. *Tellus B* 63, 129–139.
- Simoneit, B.R.T., Schauer, J.J., Nolte, C.G., Oros, D.R., Elias, V.O., Fraser, M.P., Rogge, W.F., Cass, G.R., 1999. Levoglucosan, a tracer for cellulose in biomass burning and atmospheric particles. *Atmos. Environ.* 33, 173–182.
- Szidat, S., Jenk, T., Synal, H.A., Kalberer, M., Wacker, L., Hajdas, I., Kasper-Giebl, A., Baltensperger, U., 2006. Contributions of fossil fuel, biomass-burning, and biogenic emissions to carbonaceous aerosols in Zurich as traced by ^{14}C . *J. Geophys. Res.* 111, D07206. <http://dx.doi.org/10.1029/2005JD006590>.
- Takahashi, K., Mori, I., Nishikawa, M., Quan, H., Sakamoto, K., 2008. Carbonaceous components of atmospheric aerosols in Beijing and Tokyo. *Earozoru Kenkyu* 23, 194–199.
- Turpin, B.J., Huntzicker, J.J., 1995. Identification of secondary organic aerosol episodes and quantitation of primary and secondary organic aerosol concentrations during SCAQS. *Atmos. Environ.* 29, 3527–3544.
- Wang, G., Kawamura, K., Lee, S., Ho, K.F., Cao, J., 2006. Molecular, seasonal, and spatial distributions of organic aerosols from fourteen Chinese cities. *Environmental Science & Technology* 40, 4619–4625.
- Widory, D., 2006. Combustibles, fuels and their combustion products: a view through carbon isotopes. *Combust. Theor. Model.* 10, 831–841.
- Widory, D., Roy, S., Le Moullec, Y., Goupil, G., Cocherie, A., Guerrot, C., 2004. The origin of atmospheric particles in Paris: a view through carbon and lead isotopes. *Atmos. Environ.* 38, 953–961.
- Xie, R., Seip, H.M., Wibetoe, G., Nori, S., McLeod, C.W., 2006. Heavy coal combustion as the dominant source of particulate pollution in Taiyuan, China, corroborated by high concentrations of arsenic and selenium in PM₁₀. *Sci. Total Environ.* 370, 409–415.
- Xu, H.M., Cao, J.J., Ho, K.F., Ding, H., Han, Y.M., Wang, G.H., Chow, J.C., Watson, J.G., Khol, S.D., W. T., Q. J., 2012. Lead concentrations in fine particulate matter after the phasing out of leaded gasoline in Xi'an, China. *Atmos. Environ.* 46, 217–224.
- Xu, H.M., Tao, J., Ho, S.S.H., Ho, K.F., Cao, J.J., Li, N., Chow, J.C., Wang, G.H., Han, Y.M., Zhang, R.J., Watson, J.G., Zhang, J.Q., 2013. Characteristics of fine particulate non-polar organic compounds in Guangzhou during the 16th Asian Games: effectiveness of air pollution controls. *Atmos. Environ.* 76, 94–101.
- Zhang, T., Cao, J.-J., Chow, J.C., Shen, Z.-X., Ho, K.-F., Ho, S.S.H., Liu, S.-X., Han, Y.-M., Watson, J.G., Wang, G.-H., Huang, R.-J., 2014a. Characterization and seasonal variations of levoglucosan in fine particulate matter in Xi'an, China. *J. Air Waste Manag. Assoc.* 64, 1317–1327.
- Zhang, Y.-x., Shao, M., Zhang, Y.-h., Zeng, L.-m., He, L.-y., Zhu, B., Wei, Y.-j., Zhu, X.-l., 2007. Source profiles of particulate organic matters emitted from cereal straw

- burnings. *J. Environ. Sci.* 19, 167–175.
- Zhang, Y., Li, J., Zhang, G., Zotter, P., Huang, R.-J., Tang, J., Wacker, L., Prevot, A., Szidat, S., 2014b. Radiocarbon-based source apportionment of carbonaceous aerosols at a regional background site on Hainan Island, South China. *Environ. Sci. Technol.* 48, 2651–2659.
- Zhang, Y.L., Huang, R.J., El Haddad, I., Ho, K.F., Cao, J.J., Han, Y., Zotter, P., Bozzetti, C., Daellenbach, K.R., Canonaco, F., Slowik, J.G., Salazar, G., Schwikowski, M., Schnelle-Kreis, J., Abbaszade, G., Zimmermann, R., Baltensperger, U., Prévôt, A.S.H., Szidat, S., 2015. Fossil vs. non-fossil sources of fine carbonaceous aerosols in four Chinese cities during the extreme winter haze episode of 2013. *Atmos. Chem. Phys.* 15, 1299–1312.
- Zhang, Y.L., Perron, N., Ciobanu, V.G., Zotter, P., Minguillón, M.C., Wacker, L., Prévôt, A.S.H., Baltensperger, U., Szidat, S., 2012. On the isolation of OC and EC and the optimal strategy of radiocarbon-based source apportionment of carbonaceous aerosols. *Atmos. Chem. Phys.* 12, 10841–10856.